# Comparing Predicted Performance of Anechoic Chambers to Free Space VSWR Measurements

Vince Rodriguez
NSI-MI Technologies
Suwanee, GA 30024USA
vrodriguez@nsi-mi.com

***Abstract*— Indoor antenna ranges must have the walls, floor and ceiling treated with RF absorber. The normal incidence performance of the absorber is usually provided by the manufacturers of the materials; however, the bi-static or off angle performance must also be known. In reference [1], a polynomial approximation was introduced that gave a prediction of the reflected energy from pyramidal absorber. In this paper, the approximations are used to predict the quiet zone (QZ) performance of several anechoic chambers. These predictions are compared with full wave analysis performed in CST Suite®. A 12 m wide by 22 m long with a height of 12 m chamber was analyzed at 700 MHz. The QZ performance was compared to the polynomial predictions showing a difference of less than 2.2 dB. In addition, comparisons are made with measurements of the QZ performance of anechoic chambers. Measurements performed per the free space VSWR method of three different chambers are compared with the prediction that uses the polynomials presented in [1]. The chambers are: a 18 m long by 11.5 m wide and 11.5 m in height operating from 100M MHz to 12 GHz; a 13.41 m by6.1 m by 6.1 m operating from 800 MHz to 6 GHz; and a 14 m long by 4.12 m by 4.27 m operating in the X band. The results show that the polynomial approximations can be used to give a reasonably accurate and safe prediction of the QZ performance of anechoic chambers.**

***Keywords—Anechoic ranges, RF Absorber, Numerical Methods***

## I. INTRODUCTION

RF absorber is used in indoor ranges to reduce reflection from certain areas of the range to create a free space condition for testing. Most manufacturers provide data on the normal incidence reflectivity where the absorber performance is optimized. In most applications of absorber in indoor ranges, it is important to know its bi-static reflectivity for oblique angles of incidence. In reference [1] a polynomial approximation was developed to provide a prediction of the reflected signal from pyramidal absorber of a given thickness $t$ for a given angle of incidence $\theta$. The resulting polynomial has the following form:

$$R(dB) = C_0(t) + C_1(t)\theta + C_2(t)\theta^2 + C_3(t)\theta^3 + C_4(t)\theta^4 + C_5(t)\theta^5 \quad (1)$$

Where $t$ is the electrical thickness (in terms of wavelengths) of the pyramids and $\theta$ is the angle of incidence. The polynomial is valid for $0.25 \le t \le 18$ and $0° \le \theta \le 85°$. The coefficients of the polynomial in (1) are a function of the thickness $t$. Their values are given by another set of equations. The 0th order coefficient is given by the following equation:

$$C_o(t) = -54.98 + 55.21e^{-0.7744t} \quad (2)$$

This equation is an approximation of the normal incidence performance of the absorber; which is $\theta = 0°$.

The rest of the coefficients of (1) were approximated by polynomials of a maximum 7th order. In general, the coefficients in (1) have the following form:

$$C_n = A_o + A_1 t + A_2 t^2 + A_3 t^3 + A_4 t^4 + A_5 t^5 + A_6 t^6 + A_7 t^7 \quad (3)$$

The choice of the 7th order may not be the best approach, as a high number of significant figures are required for the $A_n$ values. However, it simplifies the overall set of equations when compared with the approximation presented in [2]. The following table shows the values of the coefficients for the polynomials that describe the coefficients in equation (1). For $0.25\lambda \le t < 2\lambda$ the values are:

TABLE I. COEFFICIENTS FOR EQUATION (4): $0.25\lambda \leqslant t \leqslant 1.8\lambda$

| | $C_1$ | $C_2$ | $C_3$ | $C_4$ | $C_5$ |
|---|---|---|---|---|---|
| $A_0$ | -6.32E+00 | 7.69E-01 | -2.69E-02 | 3.51E-04 | -1.55E-06 |
| $A_1$ | 7.23E+01 | -8.66E+00 | 3.02E-01 | -3.94E-03 | 1.74E-05 |
| $A_2$ | -3.23E+02 | 3.84E+01 | -1.33E+00 | 1.74E-02 | -7.71E-05 |
| $A_3$ | 7.31E+02 | -8.67E+01 | 3.00E+00 | -3.92E-02 | 1.74E-04 |
| $A_4$ | -9.18E+02 | 1.09E+02 | -3.76E+00 | 4.92E-02 | -2.19E-04 |
| $A_5$ | 6.42E+02 | -7.63E+01 | 2.63E+00 | -3.44E-02 | 1.54E-04 |
| $A_6$ | -2.34E+02 | 2.78E+01 | -9.58E-01 | 1.26E-02 | -5.62E-05 |
| $A_7$ | 3.43E+01 | -4.10E+00 | 1.41E-01 | -1.85E-03 | 8.30E-06 |

TABLE II. COEFFICIENTS FOR EQUATION (4): $2\lambda < t \leqslant 18\lambda$

| | $C_1$ | $C_2$ | $C_3$ | $C_4$ | $C_5$ |
|---|---|---|---|---|---|
| $A_0$ | -1.39E+00 | 2.03E-02 | 7.63E-04 | -2.42E-05 | 1.63E-07 |
| $A_1$ | 3.07E+00 | -2.45E-01 | 7.31E-03 | -8.18E-05 | 3.08E-07 |
| $A_2$ | -1.23E+00 | 1.17E-01 | -3.86E-03 | 4.79E-05 | -2.01E-07 |
| $A_3$ | 1.77E-01 | -1.86E-02 | 6.46E-04 | -8.34E-06 | 3.61E-08 |
| $A_4$ | -1.00E-02 | 1.23E-03 | -4.53E-05 | 5.99E-07 | -2.62E-09 |
| $A_5$ | 4.92E-05 | -2.29E-05 | 1.05E-06 | -1.46E-08 | 6.34E-11 |
| $A_6$ | 1.51E-05 | -8.66E-07 | 2.01E-08 | -2.36E-10 | 1.10E-12 |
| $A_7$ | -3.96E-07 | 3.08E-08 | -9.25E-10 | 1.18E-11 | -5.35E-14 |

From these equations, a set of curves can be obtained to show the reflectivity of the absorber in dB versus angle for different thicknesses of absorber.

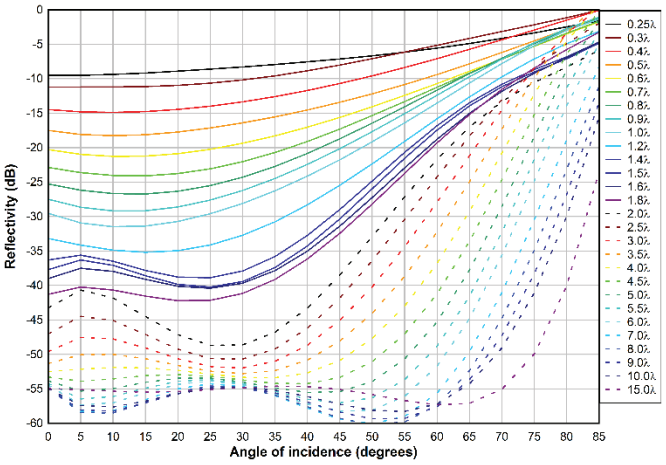


Fig. 1. Plots of the Reflectivity of RF Absorber from Equation (1)

Using these equations and the geometry of the chamber, as well as knowledge of the radiation pattern of the illuminating antenna, it is possible to estimate the highest level of reflected energy arriving into the quiet zone (QZ). That level is known as the QZ level and gives an indication of the quality of the chamber as well as an estimate of the expected measurement errors.

## II. SIMPLIFIED RAY-TRACING APPROACH

The presented approach is intended for rectangular anechoic chambers. As it will be shown, the approach is not only valid for far-field measurement ranges, but it is also valid for near-field ranges and compact ranges.

The necessary input parameters are the internal size of the anechoic chamber, length, width and height. The thickness of the absorber used on the side walls, floor, ceiling and end wall are also required parameters. The size of the QZ and the distance from its center to the source antenna are additional parameters.

There are some recommended rules for sizing a rectangular anechoic chamber. Some of these rules are given in [2-4]. A typical rectangular anechoic chamber is given in Figure 2. The chamber has an internal length (L) and height (H). The internal width of the chamber (W) is usually the same as the height (H), but this is not always the case as discussed in [2] and [4].

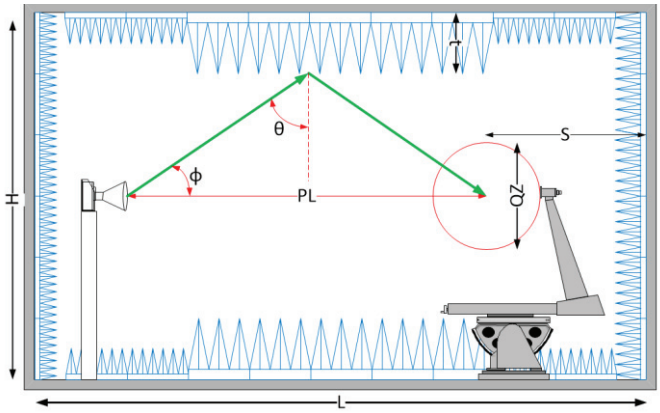


Fig. 2. Geometry of a Rectangular Anechoic Range

A simple model can be made in which only the 1st order reflections are considered. This is a very simplistic; but the goal is to achieve a simplified approach to estimate the performance of an anechoic chamber. The 1st order reflections will be the energy reflected from the end wall behind the QZ, and the reflections from the specular point in the side walls, ceiling and floor. It is assumed the source antenna has a front to back ratio high enough that the absorber on the end wall behind the source will reflect a level much lower than the other reflections. From the dimensions above the angle of incidence onto the absorber on the ceiling, floor, and the sidewalls can be calculated using basic trigonometry. This angle θ is the one used in (1) to estimate the reflected energy. For the end wall behind the QZ, equation (2) will provide the level of energy reflected.

Another factor determining the level of reflected energy entering the QZ is related to the level of energy incident onto the side walls compared to the direct path between the source antenna and the QZ. Figure 3 shows the level of the field emitted towards the specular point is about 5 dB lower than the level of the direct ray to the QZ.

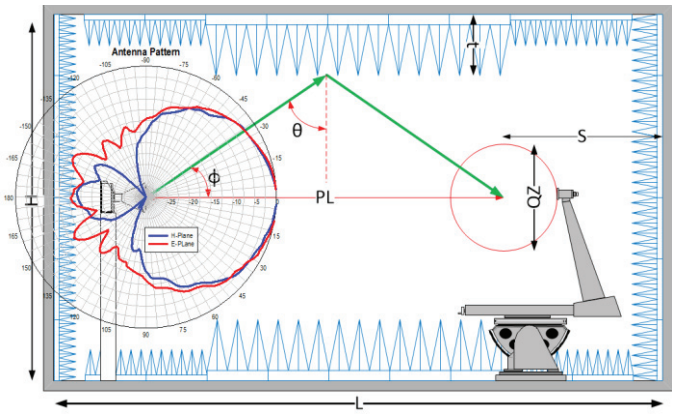


Fig. 3. A pattern of the source antenna superimposed on the chamber diagram showing that the level of energy emitted towards the specular point is lower than the level of the direct ray along the path length PL.

The difference in length between the reflected path and the direct path must be accounted. The additional losses for the longer reflected path are added to the absorber reflectivity and to the source radiation pattern difference. The path difference given by the QZ location versus the back wall is given by the distance S in Figure 3. It should be noted, when modeling compact ranges using this approach, the plane wave created by the compact range reflector will not attenuate as it propagates along the axis of the chamber. As shown in [4] the waves traveling towards the sidewalls are spherical wave fronts, not planar.

## III. Comparison with Full Wave Models

In the previous section, a very simple approach for modeling a rectangular anechoic range was presented. How good is this model? Is it good enough for estimating the performance of an anechoic range? To answer this question, two rectangular ranges will be modelled using this approach, and the performance will be compared to the computations from full wave models. CST was chosen to model the chambers. This is not a very efficient method as the required computer resources limit the highest frequency that can be computed for a given range.

### *A. A 700 MHz Large Indoor Far-Field Range*

For the far-field range, a chamber with inside dimensions of 12 m wide by 22 m long with a height of 12 m was chosen. The chamber was analyzed assuming a standard gain horn as the source antenna. The approach described in Section II was used to predict the performance of the anechoic range. The absorber layout consisted of 1m-long absorber on the receive end wall, and1.5 m-long absorber on the side walls, floor and ceiling. The other parameters for the range are as follows:

- QZ diameter is 2 m.
- The location of the QZ is 3 m from the end wall.
- The path length is set to 18.5 m.
- The frequency analyzed is 700 MHz.

For this geometry, the angle of incidence onto the side wall, floor and ceiling absorber is 64°. Equation (1) gives a reflectivity of -21.41 dB with the additional path loss of 0.8 dB for the reflected path. For the back wall, equation (2) gives us a -44 dB level with an additional 2 dB of path loss. The nominal 15.5 dB SGH (a model MI-210-0.49) has a directivity of 16.8 dB at 700 MHz and it reduces the energy illuminating the side walls by approximately -12 dB for both planes. From this analysis, the following QZ levels are estimated.

TABLE I. QZ Levels per the Simplified Model

| Frequency (GHz) | Source antenna directivity (dB) | QZ level (dB) | Amplitude ripple (dB) |
|---|---|---|---|
| 0.70 | 15.5 | -34.21 | ±0.17 |

Figure 4 shows the chamber model for the full wave analysis. The figure shows a view of the model with one wall removed for clarity. Two views are shown: one looking towards the QZ and one towards the standard gain horn (SGH) that illuminates the chamber. Notice the model shows flat absorber behind the QZ on the floor, ceiling and side walls, and that no special treatment has been done on the edges, which are bare metal exposed at the edges of the anechoic room.

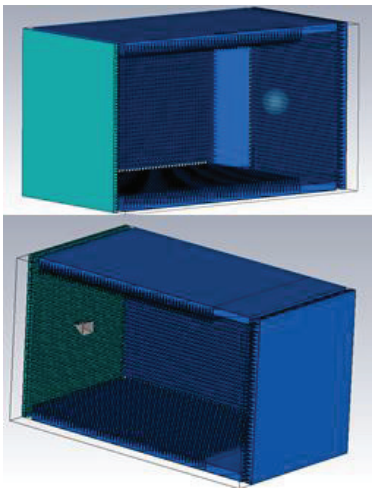

Fig. 4. Model of the Large Far-Field Chamber

The full wave analysis provides the field distribution at 700 MHz in the two orthogonal planes of symmetry of the anechoic chamber. Figure 5 shows the field distribution in the anechoic chamber in these two planes. The typical pattern of the SGH is evident in these field distributions.

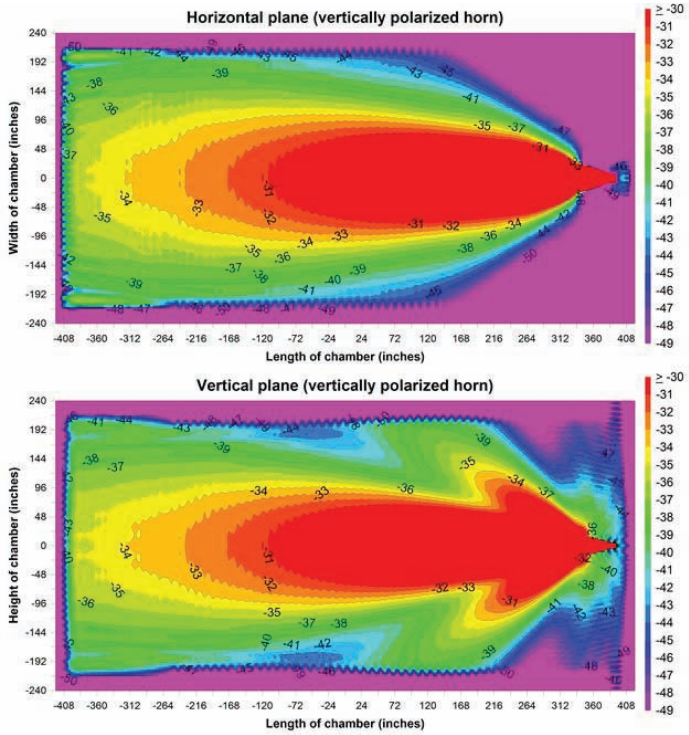


Fig. 5. Field distribution at 700 MHZ in the large far field range in the horizontal and the vertical planes. Note the SGH pattern of the source antenna.

As was done for the near-field range analyzed in Section A, the field along the three main axes of the spherical QZ are plotted, and a 2nd order polynomial fit obtained. The ripple riding on the 2nd order approximation is calculated, and from it, the reflectivity of the QZ is obtained. Figure 6 shows the longitudinal scan of the QZ with a 0.22dB peak-to-peak ripple equivalent to a -38dB level.

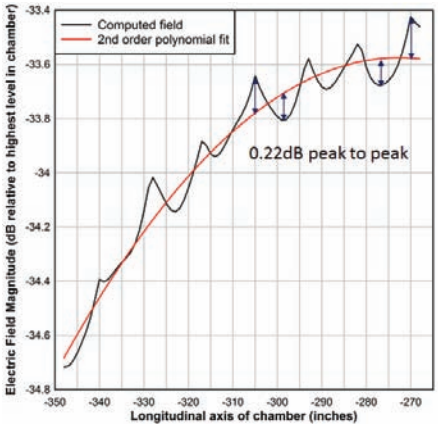


Fig. 6. Longitudinal Scan of the QZ for the Large Far-Field Range at 700 MHz

Figure 7 shows the transverse scan along the vertical axis of the QZ. The ripple is 0.26 dB peak-to-peak, which is equivalent to a -36.4 dB reflectivity.

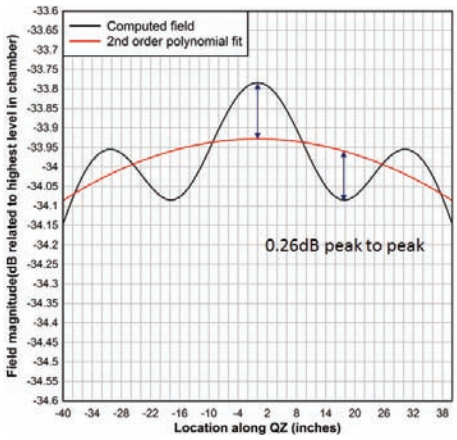


Fig. 7. Transverse Scan of the QZ along the Vertical Axis

The transverse scan along the horizontal axis shows a similar peak-to-peak ripple of 0.2 dB, which is equivalent to a reflectivity of -39 dB. The data is shown in Figure 8.

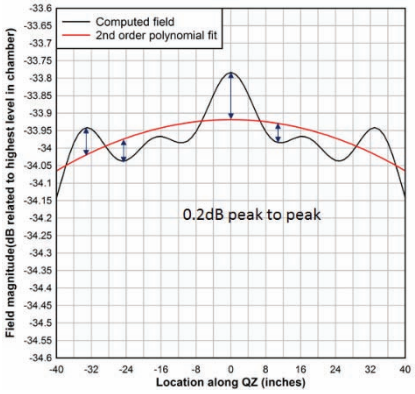


Fig. 8. Transverse Scan of the QZ along the Horizontal Axis

The data indicate that the highest reflectivity is in the -36.4 dB range. This value is extremely close to the analysis based on equation (1) which estimated a reflectivity level of -34.21 dB.

## IV. Comparison with Measurements

### *A. A 100MHz Large Indoor Far-Field Range*

To further verify the analysis approach introduced in Section II of this paper, an existing chamber is analyzed. The results of the analysis are compared with measurements done per the free space VSWR method in [5]. The anechoic chamber is 18 m long by 11.5 m wide and 11.5 m in height. The QZ is a 1 m diameter sphere. The path length is 12 m. All surfaces are treated with 1.82 m (72 in.) long pyramids except for the wall behind the source antenna, which is treated with 1.22 m (48 in.) long pyramids. The chamber was measured at 100 MHz, 400 MHz, 4 GHz and 12 GHz. An Electro-Metrics Biconical-Log Hybrid model EM-6917-1 was used to illuminate the chamber from 100 MHz to 1 GHz. A Scientific Atlanta SA-12-3.9 SGH was used for the 4 GHz measurement and a SA-12-12 SGH was used for the 12 GHz measurement. The following table shows the manufacturer's specification on gain for these antennas at the frequencies of the measurement:

TABLE II. SOURCE ANTENNA GAIN

| Antenna | Frequency | Nominal Gain |
|---|---|---|
| EM-6917-1 | 100 MHz | 1 dB |
| EM-6917-1 | 400 MHz | 6 dB |
| SA-12-3.9 | 4 GHz | 18 dB |
| SA-12-12 | 12 GHz | 24.7 dB |

The antenna pattern is estimated by assuming a square aperture with a TE01 illumination using the equations for TE01 appertures shown in [6]. The size of the apperture is adjusted to provide a pattern that has the same directivity as the gain of the antenna provided by the manufacturer. The estimated pattern is constructed by comparing the E plane and the H plane of the TE01 aperture radiation and taking the higher of the two. The constructed estimated patterns are shown in Figure 9.

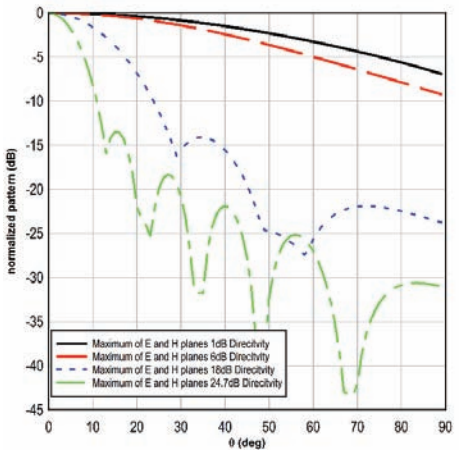


Fig. 9. Assumed Patterns used for the Analysis of the Measured Chamber

These patterns add a level of uncertainty to the QZ level estimate. This is especially the case for 100 and 400 MHz, since the actual directivity of the antenna is not known.

Based on the geometry, the absorber thickness and the estimated patterns, the following reflectivity levels are computed using the the simple ray-tracing and equation (1):

TABLE III. PREDICTED REFLECTIVITY

| Frequency | QZ Reflectivity | Amplitude Ripple |
|---|---|---|
| 100 MHz | -11 dB | ±2.84 dB |
| 400 MHz | -27 dB | ±0.38 dB |
| 4 GHz | -55 dB | ±0.02 dB |
| 12 GHz | -55 dB | ±0.02 dB |

The chamber was measured per the free space VSWR method, thus the QZ was scanned in the horizontal plane along the longitudinal and transverse axis with the probe antenna oriented at different angles. The ripple patterns obtained are used to determine the reflectivity of the QZ as described in [7]. Figure 10 shows some pictures of the measurement of the anechoic chamber.

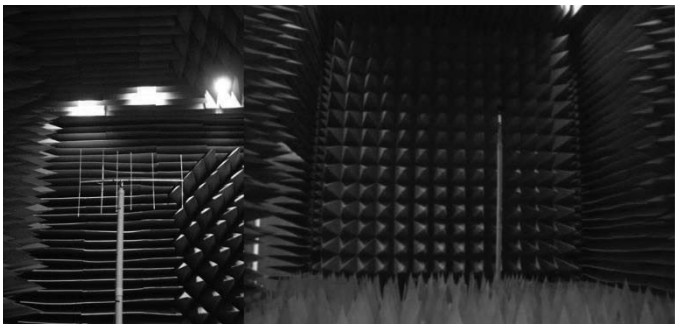

Fig. 10. Two pictures of the testing of the chamber. On the left, a large Yagi is used to scan the QZ at 100 MHz seen from the side wall of the chamber. On the right, a horn is used to scan at 12 GHz as seen for the source wall.

The following table shows the measured levels for the anechoic chamber per the free space VSWR approach:

TABLE IV. MEASURED AND PREDICTED REFLECTIVITY

| Frequency | Measured QZ Reflectivity | Predicted QZ Reflectivity |
|---|---|---|
| 100 MHz | -16.79 dB | -11 dB |
| 400 MHz | -30.88 dB | -27 dB |
| 4 GHz | -57.63 dB | -55 dB |
| 12 GHz | -52.62 dB | -55 dB |

The results in Table VI show excellent agreement with the predictions from the method that uses Equation (1). The biggest disagrement is at 100 MHz. It should be noted that there are some issues with the method presented in [5] as was recently reported in [8]. In this particular case, the quiet zone is 1 m in diameter. Hence, at 100 MHz the QZ is 1/3 λ. This seems to be too small to be able to catch any ripple due to reflected energy. Thus, the measured reflectivity may be overstimated. Some of the peaks and the valleys of the standing waves may not appear within the scanned QZ. At the other measured frequencies, the results are very close given the approximation used for the source antenna pattern.

### *B. An 800 MHz Small Indoor Far-Field Range*

As in the previous case, a 6.1 m x 6.1 m x 13.4 1 m (20 ft x 20 ft x 44 ft) chamber was manufactured and measured using the free space VSWR methodology. The chamber has a 1.98 m (6.5 ft) spherical QZ located at one end of the chamber. The chamber is lined with 91.4 cm (36-in) absorber on the end wall behind the QZ and with 1.22 m (48-in) absorber on the critical areas of the sidewalls, floor, and ceiling. The antennas used to iluminate the QZ are a log periodic antenna model EMCO 3147 and a dual ridge guide horn model EMCO 3115. The path length is 7.62 m (25 ft). Figure 11 shows views of the anechoic chamber.

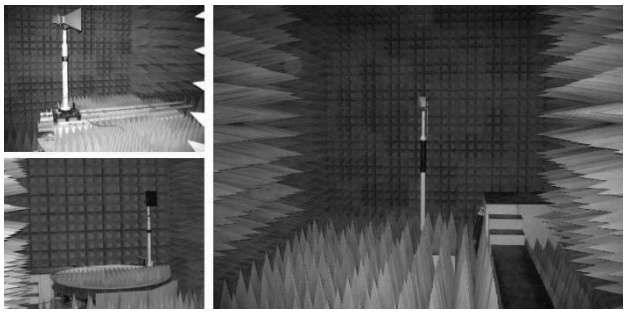

Fig. 11. Views of the anechoic chamber being analyzed.

The following table shows the comparison between the measured reflectivity and the predicted results:

TABLE V. MEASURED AND PREDICTED REFLECTIVITY

| Frequency | Measured QZ Reflectivity | Predicted QZ Reflectivity |
|---|---|---|
| 0.80 GHz | -32.21 dB | -25 dB |
| 1.80 GHz | -38.67 dB | -45 dB |
| 2.45 GHz | -47.21 dB | -50 dB |
| 6.00 GHz | -52.88 dB | -54 dB |

Given the geometry of the range, the specular reflection is at about 64°. For that angle the 48-inch absorber (3.25λ at 800 MHz) has a reflectivity of -23.88, the EMCO 3147 pattern is about 1 dB lower at 25° for the H-plane. The additonal path length only has about -0.6 dB of additonal loss, so the highest reflectivity is about -25.48 dB. For this case there is clearly a larger difference. The difference at 800 MHz cannot be explained by the fact that the QZ is too small to be able to measure the ripple, as was described in the previous case. However, it may point to other limitations or sources of error in our methodology.

The ray tracing method is an asymptotic approach. It is intended to be used when the dimensions of the structure are much larger that the wavelength. As the frequency increases, the prediction is closer to the measured reflectivity. More analysis is needed to reduce the uncertainty of the method. Unfortunately, no uncertainty analysis was provided with the test reports. In [7] some of the sources of uncertainty for the free space VSWR method were discussed.

### *C. X-band Range in a Narrow Chamber*

One last comparison was made for a 12 m long (40 ft) by 4.12 m (13.5 ft) tall by 4.27 m (14 ft) wide chamber. The chamber is lined with 12-inch absorber on the side wall and 8-inch on the end wall behind the 1.2 2m (4 ft) QZ. The angle of incidence onto the side wall absorber is 71°, and it is 72° on the floor and the ceiling. The chamber is illuminated with an X-band 21 dBi horn from Rozendal Associates Incorporated. The measured QZ reflectivity at 10 GHz per the free space VSWR method is -55.16 dB, while the prediction from the analysis is -54 dB. So, for electrically large chambers the results are good, even when there is an extremely large angle of incidence.

## V. CONCLUSIONS

The results presented have shown that the simplified ray-tracing approach, together with the equations introduced in [1], provide a good approach to estimating the performance of an anechoic chamber. This approach has been validated by comparing it to estimates from full wave analysis performed using commercially available software packages. Comparison with measured performance has also shown the approach to be valid in predicting anechoic range performance of rectangular chambers for electrically large anechoic rooms. For a smaller room, the results seem to be extremely conservative when compared to the measured results. However, the short comings of the free space VSWR method discussed in [8] should be considered. The data presented in this paper increases the confidence on the equations introduced in [1] for the prediction of pyramidal absorber reflectivity.

## REFERENCES


[1] V. Rodriguez and E. Barry, "A polynomial approximation for the Prediciotn of Reflected Energy from Pyramidal RF Absorbers," *Proceedeings of the 38th annual Symposium of the Antenna Measurement Techniques Association (AMTA 2016)*, pp. 155–160, October 2016.

[2] V. Rodriguez " Basic Rules for Anechoic Chamber Design, Part One: RF Absorber Approximations" *Microwave Journal*, Vol 59, No 1, pp 72-86

[3] Hemming L. *Electromagnetic Anechoic Chambers: A fundamental Design and Specification Guide* 2002 IEEE Press/Wiley Interscience: Piscataway, New Jersey.

[4] V. Rodriguez " Basic Rules for Anechoic Chamber Design, Part Two: Compact Ranges and Near Field Measurements" *Microwave Journal*, Vol 59, No 2, pp 80-90.

[5] University of Michigan Report 5391-1-F, February 1963.

[6] W. Stutzman and G. Thiele *Antenna Theory and Design* 2nd ed. John Wiley and Sons: New Yor, New York , 1998.

[7] B. Tian "Free Space VSWR Method for Anechoic Chamber Electromagnetic Evaluation" *Proceedeings of the 30th Annual Symposium of the Antenna Measurement Techniques Association (AMTA 2008)*, pp. 524–529, November 2008.

[8] Z Chen, Z. Xiong, and A. Enayati " Limitations of the Free Space VSWR Measurements for Chamber Validation" *Proceedings of the 38th annual Symposium of the Antenna Measurement Techniques Association (AMTA 2016)*, pp. 144–148, October 2016.